Mechanical properties of thermally sprayed porous alumina coating by Vickers and Knoop indentation

Ghailen Ben Ghorbal, Arnaud Tricoteaux, Anthony Thuault, H. Ageorges, F. Roudet, D. Chicot

Mechanical properties of thermally sprayed porous alumina coating by Vickers and Knoop indentation

G. Ben Ghorbal[a,b], A. Tricoteaux[a], A. Thuault[a], H. Ageorges[c], F. Roudet[d], D. Chicot[d,*]

[a] Univ. Polytechnique Hauts-de-France, EA 2443 – LMCPA – Laboratoire des Matériaux Céramiques et Procédés Associés, F-59313, Valenciennes, France
[b] PIMM, Arts et Métiers ParisTech/CNRS/CNAM, 151 Boulevard de l'Hôpital, 75013, Paris, France
[c] Univ. de Limoges, IRCER, UMR CNRS 7315, 12 Rue Atlantis, 87000, Limoges, France
[d] Univ. de Lille, Laboratoire de Génie Civil et Géo-Environnement, LGCgE EA1445, 59650, Villeneuve d'Ascq, France

Keywords:
Instrumented indentation
Knoop and vickers hardness
Mechanical properties
Plasma spray
Alumina coating

A B S T R A C T

Depending on the thermal spraying conditions, coatings obtained can present different defects, like pores, cracks and/or unmelted particles, and different surface roughnesses, that can affect the determination of the hardness and elastic modulus. The present work investigates the mechanical properties, determined by means of Knoop and Vickers indentations, of a plasma as-sprayed alumina coating, obtained with a nano-agglomerated powder sprayed using a PTF4 torch, in order to highlight how the surface defects interfere into the indentation process. As a main result, Knoop indentation compared to Vickers one gives less dispersive results (15% and 33%, respectively), that are, in addition, more representative of the coating properties. The mean values obtained are 110 ± 40 GPa for the elastic modulus and 1.75 ± 0.42 GPa for the hardness. In addition, and for the two indenter types used, multicyclic indentation has been performed because it allows a more appropriate characterization of such heterogeneous coatings due to the representation of the mechanical properties as a function of the indentation load and/or the penetration depth, leading to more reliable results according to the depth-variability of the coating microstructure.

1. Introduction

Porous materials are of great industrial interest because they combine the usual properties of ceramic materials, such as chemical stability, thermal insulation capacity, and wear resistance, to multifunctional properties such as lightness, great exchange surface promoting chemical or biological reactions [1–5]. They may be in bulk form or in the form of coating deposited onto a substrate to improve a desired performance. However, the porosity and/or the substrate can influence the determination of the mechanical properties of such highly heterogeneous materials [6–8], which are often determined on the polished cross section in the case of coatings [9–13]. Thus, it is essential to be able to characterize them reliably and when possible without preparation of the sample.

Instrumented indentation techniques have been consistently developed in recent decades to evaluate the mechanical properties of most materials ranging from bulk materials to thin or thick coatings, and from homogeneous to highly heterogeneous materials. Interest of instrumented indentation test (IIT) is that it allows evaluating the local properties of phases constituting a material or coatings by avoiding the influence of the substrate depending on the scale of measurement. The non-destructive nature and simplicity of implementation of these techniques are the main advantages that make of the indentation test a conventional technique to evaluate the hardness and elastic modulus of materials, particularly coatings. This technique has also been found useful for assessing toughness from crack length measurements generated along the diagonals of the indentation imprint [10,14,15]. Indeed, the sharp indenters commonly used in instrumented indentation, such as Vickers and Berkovich indenters, generate cracking of the material [16–18], or fail to overcome the influence of the substrate of the coated materials, sometimes even at very low loads [13,19,20]. The Knoop indenter has a more elongated and less acute shape than the Vickers and Berkovich indenters, which makes it possible to solicit a larger surface while sinking less and thus limiting the cracking under indentation of the material [16–18]. However, the use of the Knoop indenter in instrumented indentation presents an obstacle related to its less symmetrical diamond shape than the other ones. Recently a methodology to take into account the anisotropic elastic recovery in the residual imprint of Knoop indentation has been developed [16]. This method leads to comparable elastic moduli than those obtained by

* Corresponding author.
E-mail address: didier.chicot@univ-lille.fr (D. Chicot).

using Vickers indenters on dense ceramic materials. In the present work, this method is used to evaluate its validity in the specific case of porous thermally as-sprayed coating.

2. Material and experimental techniques

2.1. Plasma spraying of Al_2O_3 coating

The alumina coating under investigation has been manufactured by Atmospheric Plasma Spraying (APS) with a conventional direct current plasma gun PTF4 from Sulzer Metco. The feedstock used was a nanometric α-Al_2O_3 powder with a particle size ranging between 200 and 500 nm agglomerated into 25–100 μm (d_{50} = 55 μm) grain size. The powder was injected perpendicularly to the plasma jet axis. The powder was sprayed onto a low carbon steel (C40) as substrate. This last one was firstly grit blasted with corundum alumina then cleaned in an acetone bath with ultrasonic stirring in order to increase the mechanical anchorage of the sprayed particles. The resulting substrate surface roughness was 5.3 ± 0.1 μm. Before spraying, the substrate was preheated at 300 °C, with the plasma gun without powder feeding, to improve the adhesion of the coating. Then, during spraying, this surface temperature was maintained around 300 °C and continuously monitored by an infrared monochromatic pyrometer which controlled the cooling air rate, in order to reduce the residual stress in the coating. The plasma jet parameters used are presented in Table 1.

The microstructure and the topography of the obtained coating were examined complementarily using a scanning electron microscope (SEM) Hitachi S3500 N and Leica DCM 3D confocal profilometry.

2.2. Instrumented indentation test

2.2.1. Experimental test

Microindentation tests were performed with a micro-hardness Tester CSM 2-107 equipped with Vickers and Knoop indenters. The maximum loads were chosen within the range 500 mN to 20 N. The duration of the test is kept constant at 1 min and 15 s, including loading in 30 s, holding for 15 s and unloading in 30 s. Therefore, loading and unloading speeds are imposed proportionally to the maximum load as recommended by ISO14577: 2015 [21].

Fig. 1 shows some characteristic indentation curves using Vickers indenter (a) and Knoop indenter (b). Tests were conducted on the top surface of the as-sprayed alumina coating. One can notice a great variability of the curves with a presence of several shifts called pop-in, due to sudden depression of the indenter. This phenomenon may be due to the collapse of the material under the indenter and/or the presence of porosity or the formation of cracks under the indenter. Authors [9] have also shown that, in the case of coatings obtained by thermal spraying, this phenomenon can be related to the collapse of roughness.

Table 1
Plasma spraying parameters used to obtain the alumina coating deposited onto a low carbon steel substrate and physical properties of the coating.

Plasma Parameters	Unit	Value
Substrate temperature	°C	300
Arc current	A	500
Electric power	kW	36.5
Argon flow rate	slm	45
Hydrogen flow rate	slm	15
Spray distance	mm	100
Spray rotation speed	m/s	1
Powder flow rate	g/min	30
Argon carrier gas flow rate	slm	5
Coating physical properties		
Average coating thickness	μm	80 ± 8
Porosity	%	5.4 ± 0.8
Surface roughness	μm	10.5

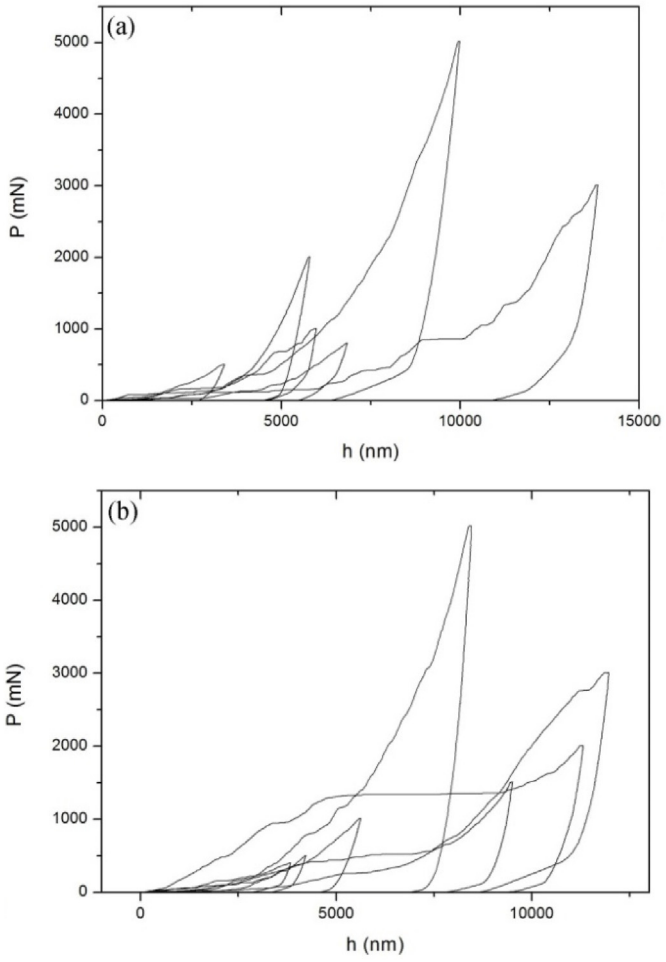

Fig. 1. Instrumented indentation curves with Vickers indenter (a) and Knoop indenter (b) obtained on as-sprayed alumina coating.

These authors also mention that this kind of curve obviously leads to a great dispersion of the hardness and elastic modulus. Additionally, to avoid such phenomena, Miller et al. [22] indicate that the penetration depth should be at least 5 times the Ra roughness.

It is therefore illusory to imagine that these indentation curves make possible to obtain reliable results and thus to compare the results obtained by the two types of indenters. In order to minimize the errors related to the roughness influence, it is obvious that one solution could be the polishing of the sample before testing. However, by an instrumented indentation analysis of the same type of coating with and without polishing, Chicot et al. [9] showed that the hardness measured on the polished surface is on average 30% greater than that measured on the unpolished surface. They also showed that the results dispersion is in the same order of magnitude. The authors concluded that the polishing of such coatings does not lead to a better results dispersion, but modifies the properties of the coating by filling the surface porosity. Alternative solution could be also the use of higher indentation loads, in the macro-loads range by using an instrumented macroindenter. However, under these loading conditions, the substrate will be as more influent that the load is higher, and possibly, the mathematical models used to separate the contribution of the substrate in the hardness measurement could led to wrong values of the mechanical properties. That is why in this work the coated material is studied as it is, without any polishing prior to the mechanical characterization. It should also be noted that the testing conditions are performed on materials which are finally under their conditions of use in service.

Alternatively, to classical instrumented indentation test, multicyclic

indentation tests were performed, which allows to obtain after each cycle the mechanical properties as a function of the indenter penetration depth. In order to limit the effect of cycling on the mechanical properties measurement which could be related to fatigue indentation test, the number of cycles has been limited to 100 cycles. Additionally, multicyclic indentation test can be performed by applying a constant indentation load at the same location or by applying increasing loading between minimum and maximum loads. As an example, Jankowski et al. [23] shown that under constant multicyclic indentation loading applied to a massive Lead-Sean eutectic material after 1000 cycles, the indentation depth increases following a Manson-Coffin law representative of a fatigue behavior of their material. To avoid such fatigue influence, only 100 cycles have been applied and additionally using increasing loading mode thus reducing the effect of fatigue cycle since the depth increases following the supplement of load compared to the previous one and not to a plastic accommodation of the material under the same load. This type of test has been successfully used and described [24,25] for the characterization of massive materials and thermally sprayed coatings.

However, when studying mechanical properties of coatings from their surface, the substrate can interfere on the mechanical properties measurement. From a general point of view for harder coatings deposited onto softer substrates, the substrate influences the measurement when the indentation depth is higher than 10% of the coating thickness for hardness measurement and only 1% for elastic modulus measurement [19]. In this case, elastic modulus and hardness should varied from the values of the coating toward those of the substrate when the depth increases, and subsequently for higher loads. In this case, two options arise: i) the mechanical properties kept constant for the lowest indentation depths thus indicating that only the mechanical properties of the coating were determined, there is no influence of the substrate, and ii) the mechanical properties vary after a plateau for the lowest indentation loads from the values of the coating toward those of the substrate. In this second situation, a variation a large variety of models exist and must be applied to separate the two contributions of the substrate and of the coating [19]. Finally, the experimental results only will discriminate the two cases and, consequently regarding the obtained results, the appropriate methodology will be applied.

In this work, the maximum load applied in the first cycle was 500 mN and, in the last one, was 20 N. Five tests with each indenter (Vickers and Knoop) at five different locations on the surface of the as-sprayed coating were performed. A multicyclic test is carried out at the same location on the surface and the progressive increase of the load has the effect of limiting the abrupt collapse of the material and therefore the pop-in effect. Fig. 2 presents the curves obtained by multicyclic indentation using a Vickers (Fig. 2a) and a Knoop indenter (Fig. 2b) on the as-sprayed plasma alumina coating studied in the paper.

It is noticeable from Fig. 2 that incremented cyclic indentation makes possible to limit the phenomena of pop in, whatever the indenter used, compared to the indentation curves presented Fig. 1.

2.2.2. Indentation background theory

The hardness computation is defined by the ratio between the indentation load and a representative contact area. Subsequently, the hardness number can be calculated considering the true or projected contact area calculated considering the maximum or the real contact depth between the indenter and the material. Mainly two hardness numbers are employed: The Martens hardness, $H_{M,}$ considers the maximum indentation depth and the true contact area whereas Instrumented hardness, H_{IT}, takes into account the contact depth between the indenter and the material and the projected contact area. Thus H_{IT} which is considered in this work is expressed by the ratio between the maximum applied load P_{max} and the projected contact area between the indenter and the indented material A_c which is computed applying the methodology developed by Oliver and Pharr [26,27]. In this condition, hardness H_{IT} is expressed as a function of the projected contact area A_c:

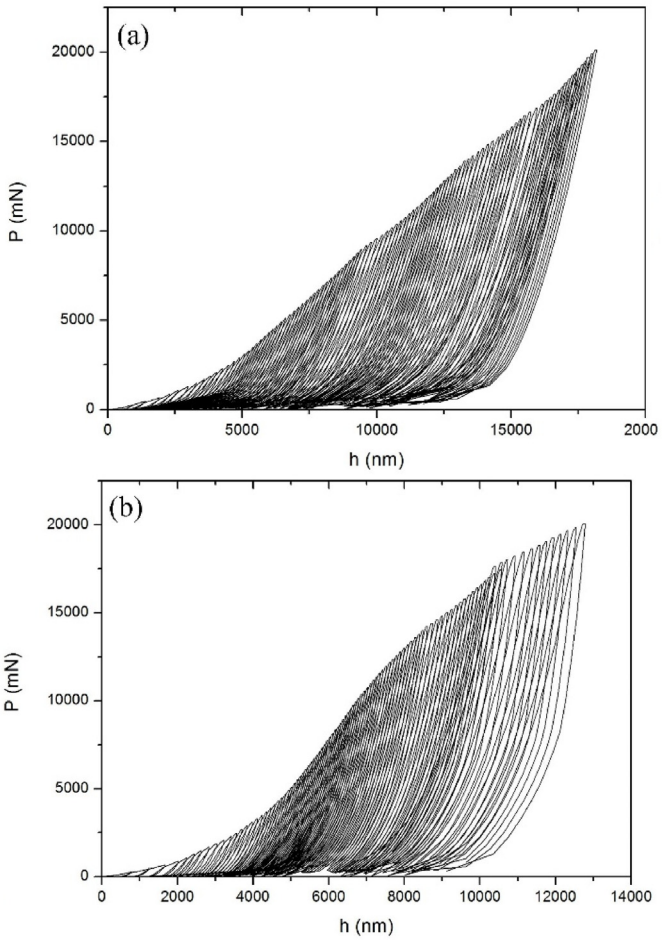

Fig. 2. Cyclic indentation curves obtained on as sprayed plasma Al_2O_3 coating using a Vickers indenter (a) and a Knoop indenter (b).

$$H_{IT} = \frac{P_{max}}{A_c} \tag{1}$$

Depending on the geometry of the indenter used, the projected contact area A_c is expressed for a perfect indenter as a geometrical function of the contact depth h_c as follows:

$$A_c = k \cdot h_c{}^2 \tag{2}$$

where k is equal to 24.5 and 65.4 for Vickers and Knoop tip respectively.

From each unloading part of the load-indentation displacement curve, the reduced elastic modulus E_r can be determined by applying the methodology originally proposed by Sneddon [28] expressed as:

$$E_r = \frac{\sqrt{\pi}}{2\beta\gamma}\frac{S}{\sqrt{A_c}} \tag{3}$$

where β, equal to 1.05, is a geometrical correction factor associated to the indenter used and γ is related to the elastic recovery occurring in the residual imprint as it was reported by Hay et al. [29]. In previous work [30], it was shown that the factor γ such it is defined by Hay et al. [29] is not appropriate for Knoop indentation due to the anisotropic elastic recovery occurring on the residual imprint [16,31,32]. In order to correct the unusual elastic recovery in Knoop indentation, the proposed correction is:

$$\gamma = \frac{h_m}{h_c} \tag{4}$$

Where h_m is the maximal indentation depth and h_c is the contact depth. In Vickers indentation this factor is a constant equal to 1.09 when considering the value of 0.3 for the Poisson's ratio of the coating [30].

The reduced elastic modulus E_r is an equivalent elastic modulus that takes into account the elastic modulus and Poisson's ratio both of the indented material and of the indenter, E, ν, E_i and ν_i, respectively.

$$\frac{1}{E_r} = \frac{(1-\nu^2)}{E} + \frac{(1-\nu_i^2)}{E_i} \tag{5}$$

The contact depth (Fig. 2b) is determined as proposed by Oliver and Pharr [25,26]:

$$h_c = h_m - \varepsilon\frac{P_{max}}{S} \tag{6}$$

ε is a constant parameter equal to 0,75 [33]. The contact stiffness S is determined from the slope of the unloading part of load-displacement curve $S\left(S = \left(\frac{dP}{dh}\right)_{h=h_m}\right)$.

The displacement sensor considers any deformation of the instrument during the test as a displacement into the sample, depending on the instrument generation. Therefore, the value of the measured compliance $1/S$ includes a contribution of the frame compliance C_f of the instrument:

$$\frac{1}{S} = \frac{\sqrt{\pi}}{2}\frac{1}{\beta\gamma E_r\sqrt{A_c}} + C_f \tag{7}$$

Frame compliance C_f has to be subtracted in order to obtain the compliance of the specimen sample and reliable measurements of elastic modulus [33]. Eq. (7) shows that the apparent frame compliance can be determined for each series of indentation experiments as the intercept of the straight line obtained by plotting the total compliance $1/S$ versus $1/\sqrt{A_C}$. The reduced elastic modulus can be easily determined from the slope of the straight line obtained.

3. Results and discussions

3.1. Microstructure and topography of the alumina coating

The microstructure of the plasma sprayed Al_2O_3 coating was examined using a scanning electron microscope on the as-sprayed surface (Fig. 3a and b) and the polished cross section (Fig. 3c and d).

These micrographs show that the Al_2O_3 coating is very porous and heterogeneous, with denser areas than others and a non-uniform pores distribution (Fig. 3d). The coating presents cracks in the entire cross section (Fig. 3d). The presence of agglomerates and some unmelted particles on the surface is exhibited (Fig. 3b). It can be noticed that the agglomerates present on the surface significantly increase the surface roughness because they are not melted in the plasma jet and then they are not well spread at the impact on the coating in formation (Fig. 3b and d). The thickness of the coating is very variable (Fig. 3c). The average thickness of the Al_2O_3 coating was determined by SEM image analysis from five images obtained at five different locations in the cross section of the coating. The average coating thickness measured is 80 ± 8 µm. The porosity rate of the coating was also evaluated by image analysis. Five analyzes were carried out on the cross-section and the porosity rate was found in the average value of 5.4 ± 0.8%. Fig. 4 shows the topography of the coating obtained with confocal profilometry. The measured arithmetic roughness Ra of the surface is about 10.5 µm.

3.2. Mechanical properties

3.2.1. Frame compliance

It has been previously shown that the raw data obtained at the end of each test requires consideration of the frame compliance. In the case of coatings, it is also necessary to verify whether there is an influence of the substrate on the determination of frame compliance [34]. Fig. 5a and b shows the evolution of the total compliance $1/S$ as a function of $1/\sqrt{A_C}$ obtained for the tests carried out using the Vickers indenter and the Knoop indenter. It is highlighted that this evolution can be represented by a straight line for all the tests, which means that there is no influence of substrate on the determination of the frame compliance. The frame compliance can therefore be determined as in the case of a bulk material.

The same observation was reported by Mejias et al. [24] by conducting incremented indentation tests on hydroxyapatite coatings deposited by thermal spraying onto steel substrates. Łatka et al. [35] also showed by instrumented indentation of thermally sprayed zirconia coatings that this phenomenon is due to the fact that the coating has an elastic modulus lower than that of the substrate. For the authors, this is a typical behavior of soft coatings on harder substrates [36]. In this study, for the tested materials, the coating present lower elastic modulus than that of the substrate as it is shown below.

Table 2 presents the instrument compliance values calculated for all

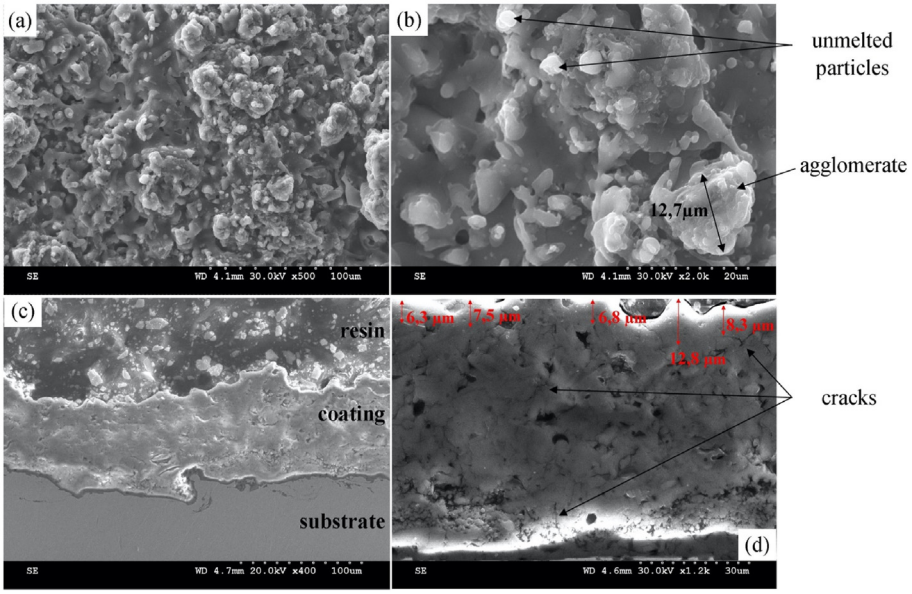

Fig. 3. Microstructure of the plasma sprayed Al_2O_3 coating at surface (a and b) and at cross section (c and d).

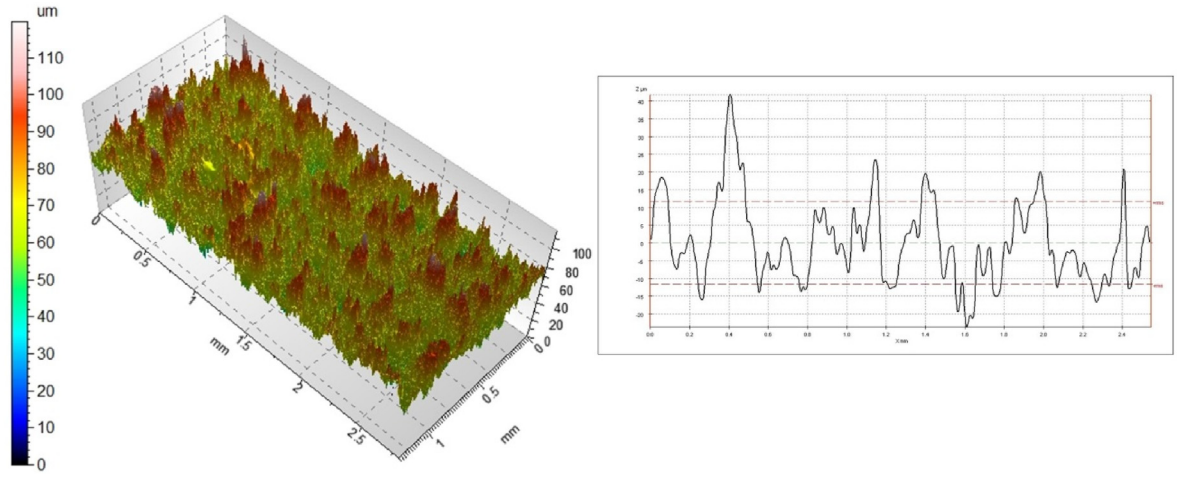

Fig. 4. Surface topography of the as sprayed Al_2O_3 plasma coating obtained by confocal profilometry.

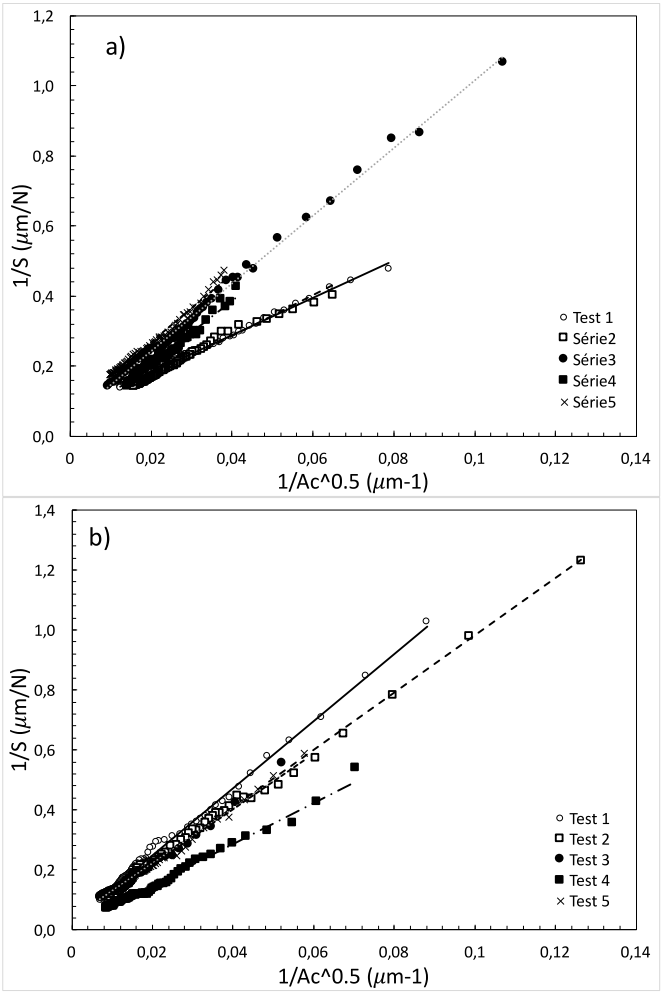

Fig. 5. Evolution of the total compliance 1/S versus $1/\sqrt{A_C}$ in the case of Vickers (a) and Knoop (b) multi-cyclic indentation tests.

tests performed.

It is exhibited that the value of C_f is different from one test to another and from one indenter to another. The same result was reported in many papers [34,37]. This confirms that the frame compliance should be taken into account for each series of measurement. This result leads to a questioning on the real parameters implied into the frame compliance measurement. Depending on how the indenter displacement is measured by the instrument, different parameters can affect the frame compliance computation as, for example, the sample mounting, the indenter fixing and design, the loading conditions, …That is why the companies have realized a great effort to minimize influence of such parameters on the mechanical properties calculations through the frame compliance. In this work, the CSM instrument is of first generation, that is why systematically it is recommended to perform the determination of the frame compliance to obtain reliable data. In any case, it is suggested applying this methodology to correct the raw data if necessary.

Table 2
Values of the instrument compliance C_f obtained with the two types of indenters.

Test	C_f *(μm/N)* Vickers	C_f *(μm/N)* Knoop
1	0.076 ± 0.001	0.023 ± 0.002
2	0.055 ± 0.002	0.027 ± 0.001
3	0.051 ± 0.002	0.039 ± 0.001
4	0.028 ± 0.004	0.012 ± 0.001
5	0.074 ± 0.002	0.032 ± 0.001

3.2.2. Elastic modulus

Afterwards, to calculate the elastic modulus following Eq. (5), the elastic properties of the diamond indenter are needed, 0.07 and 1140 GPa for the Poisson's ratio and the elastic modulus, respectively. In the case of the Knoop indentation, the coefficient γ is estimated by eq. (4). This gives a mean correction coefficient γ for the five Knoop tests equal to 1.16 ± 0.01.

Since it was considered that there is no influence of the substrate on compliance, the elastic modulus can be determined from the slope of the linear regression line shown in Fig. 5a and b. However, a break in the slope was sometimes noticed whether in Vickers indentation or Knoop indentation. For example, the Vickers indentation test 2 and the Knoop indentation test 1, at about 6 μm depth. This break in slope systematically induces a decrease of the elastic modulus value. Fig. 6 shows the evolution of the elastic modulus obtained for these two tests. It is highlighted in this figure that there is a decrease of the elastic modulus at about 6 μm for both cases, then a stabilized plateau at a value of about 150 GPa for the Vickers test and 75 GPa for the Knoop test. The rupture of the slope observed does not therefore represent an influence of the substrate that has a greater elastic modulus (around 200 GPa for steel). This rupture being observed at approximately the same penetration depth of 6 μm is apparently due to the roughness of the coating (Ra = 10.5 μm) since the roughness is due to the unmelted

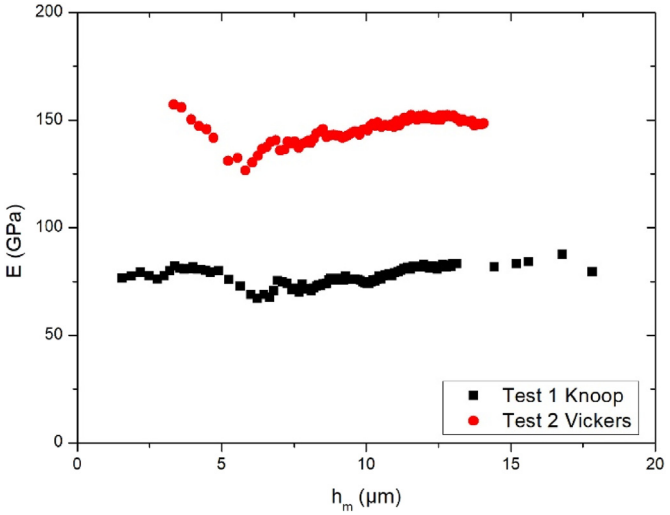

Fig. 6. Evolution of the elastic modulus obtained by multi-cyclic indentation (a) Vickers and (b) Knoop as a function of the indentation depth h_m.

agglomerates that are not as well spread as than the core of the coating (Fig. 3b and d). This is probably why the module is higher before 6 µm in depth for the two tests presented.

Therefore, the elastic modulus can sometimes increase if the indenter encounters a denser area or decrease if it encounters pores or cracks (Fig. 2d), or even if it cracks the material. However, the average value can be determined from the slope of the straight-line $1/S = f\ (1/\sqrt{A_C})$ (Fig. 5a and b) since any influence of the substrate in the obtained depth range was exhibited. Table 3 shows the average values of the elastic modulus obtained for each test using the Vickers ($E_{Vickers}$) and Knoop (E_{Knoop}) indenters.

It can be noted that the values obtained are very variable whether in Vickers or Knoop indentation. This is due to the remarkable heterogeneity of the coating. The results dispersion is more important for Vickers indentation tests since dispersion reaches 37% whereas it is 13% for Knoop indentation. This may be due to the high roughness of the coating. The Knoop indenter solicits a projected maximum area approximately 20% larger than that obtained using a Vickers indenter, at the same load [16–18]. It therefore incorporates more agglomerates on the surface and porosity, which has the effect of averaging a little more the measurements.

The Knoop measurements are also comparable to the measurements obtained on bulk alumina sample with a comparable porosity rate. Indeed, we also measured the Young modulus of a partially sintered bulk alumina with 35% porosity by instrumented Knoop indentation. We obtained comparable results of 91 ± 13 GPa in accordance with the work of Gregorová et al. [38] whom also obtained an elastic modulus of 90 GPa on a solid sample of alumina with 35% porosity.

3.2.3. Hardness

In order to validly compare the effect of the indenter shape on the mechanical properties measurement, especially for hardness calculation, the hardness definition must be at least the same. However, in practice Vickers Hardness, noted HV, is defined by the ratio of the load on the actual contact area theoretically calculated from the geometrical dimensions of the indenter (tip angle) and the diagonal of the indent measured in the plan of the material. On the other hand, Knoop Hardness, noted HK, considers the projected contact area calculated from the two tip angles of the indenter and only the large diagonal measured in the plan of the material. It is then obvious that the two hardness numbers cannot be valuably compared accordingly to these different definitions. Moreover, in instrumented indentation this is the indentation depth which is measured instead of the indent diagonal in classical tests and a simple geometrical relationship between depth and diagonal is not necessarily obvious and/or direct. That is why in the following the hardnesses are named as HP_V and HP_K instead of HV and HK, respectively, to avoid any confusion between the hardness calculated in this work and the well-known Vickers and Knoop hardness definition.

Moreover authors [30,39] suggest that it is necessary to consider the same area used in the calculation of hardness numbers, determined with different indenters, in order to compare the same entity. In fact, previous studies [16,30] showed that it is wise to consider the projected residual area in hardness calculation in order to compare hardness numbers obtained using Knoop and Vickers indenters. In this case, hardness number considering the projected residual area obtained with instrumented indentation can be calculated as follow:

$$HP = \gamma \cdot H_{IT} \tag{8}$$

where H_{IT} is calculated with Eq. (1). The hardness numbers obtained with Knoop and Vickers indenters are noted HP_K and HP_V, respectively.

In order to determine the hardness of the coating and with the objective to compare the hardness obtained by the two types of indenter, the hardness HP was calculated according to Eq. (8). Fig. 7 shows the evolution of HP as a function of the depth reached h_m for the 5 tests carried out using the Vickers indenter (Fig. 7a) and the Knoop indenter (Fig. 7b).

It can be noted in Fig. 7 that there is a high variability for the hardness values, whether in Knoop or Vickers indentation, particularly for penetration depths lower than approximately 10 µm, which is of the same order of magnitude as the surface roughness Ra. Therefore, it seems that the surface roughness of the coating significantly influences the Vickers and Knoop hardness values obtained with the two indenter types. The dispersion of the results can also be influenced by the fact that the indenter encounters a porosity on the surface of the coating or during its penetration. When the porosity is at the surface, the surface hardness will be very low as the case of the Vickers indentation tests 4 and 5. When the indenter encounters a porosity or crack during its penetration, the hardness decreases considerably, as in the case of the Vickers indentation test 4 and Knoop indentation test 2. At the same time, the incremented loading, in the same place, causes a densification of the material under the indenter. Therefore, an increase in hardness may be visible at some point in the hardness profile such as Vickers indentation test 4 and Knoop indentation test 2.

It is important to note that, globally, the hardness obtained with both types of indenter decreases as penetration depth increases, which can be associated with a very complex indentation size effect (ISE) phenomenon [40]. However, this ISE phenomenon does not seem to be related to the substrate influence since it has a hardness of about 2 GPa, which is higher than the values measured for the deeper measurements. The same hardness profile dispersion of thermally sprayed coatings has been found by several authors [9,12,24]. The authors attribute the large dispersion to the heterogeneity and roughness of thermal sprayed coatings. Therefore, an intrinsic hardness value of the coating cannot be obtained, even by applying the ISE models developed until today, since hardness varies as the indenter penetrates (deformation of roughness, compaction of the material).

However, the average was calculated for values obtained from the five tests performed with each indenter. The average values are equal to

Table 3
Elastic moduli obtained by Vickers and Knoop multicyclic indentation.

Test	$E_{Vickers}$ (GPa)	E_{Knoop} (GPa)
1	159 ± 6	78 ± 4
2	142 ± 5	90 ± 4
3	82 ± 4	80 ± 4
4	88 ± 4	110 ± 7
5	82 ± 3	82 ± 3
Average	111 ± 37	88 ± 13

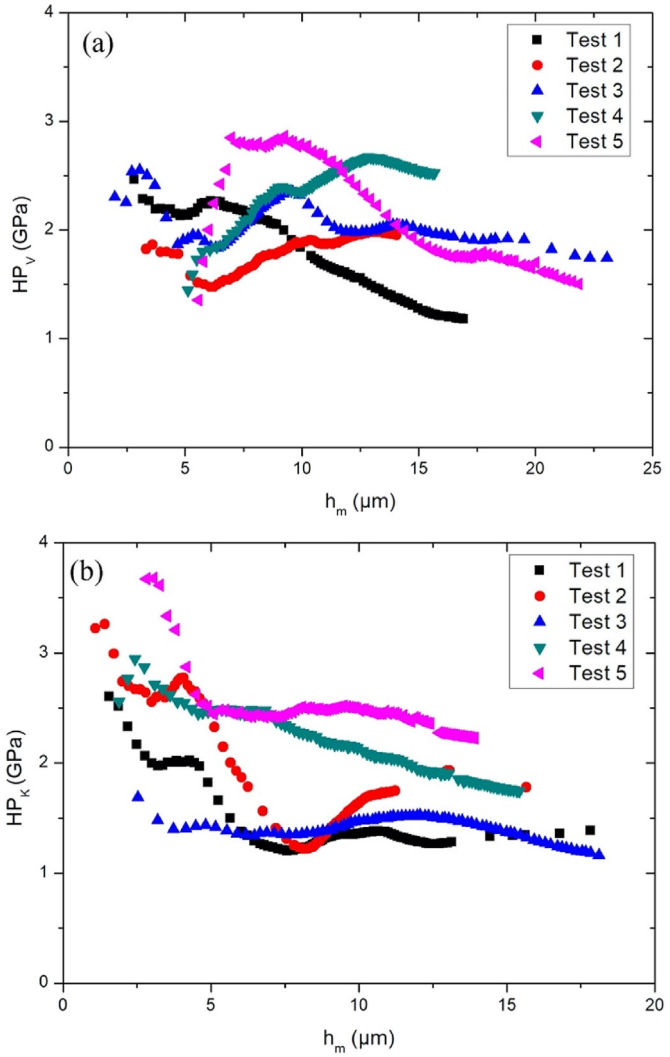

Fig. 7. Variation of the hardness HP as a function of the maximum indentation depth h_m in multicyclic (a) Vickers and (b) Knoop indentations.

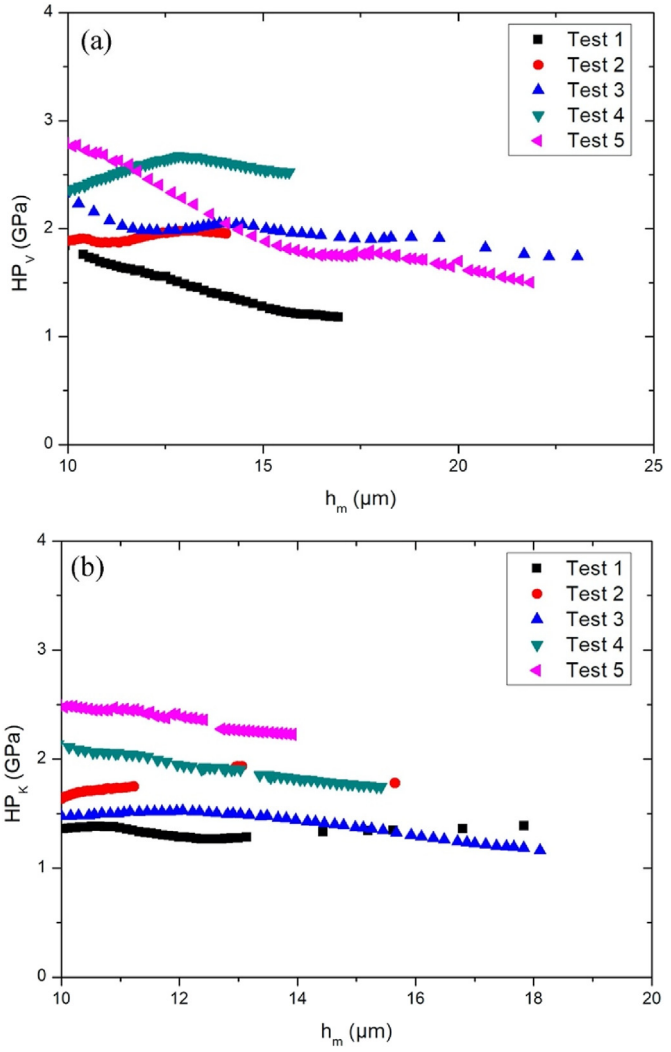

Fig. 8. Variation of the hardness HP beyond 10 μm depth in multi-cyclic indentation (a) Vickers and (b) Knoop.

2.04 ± 0.26 GPa and 1.93 ± 0.53 GPa for HP_V and HP_K, respectively. It can be noted that the average values obtained by the two types of indenters are comparable and of about 2 GPa. It is important to note that, although the value of 2 GPa is close to the hardness of the C40 substrate, there is no significant influence of the substrate in both cases, since the hardness value measured can fall below 2 GPa on the profile obtained in Fig. 7. This remains a statistical comparison between the measurements obtained by the two types of indenter. Recently, Chicot et al. [9] also showed large variations in hardness of thermally sprayed zirconia coating. In this case, they proposed to determine an average hardness at different depth intervals. So, it is proposed here to compare the average hardness beyond a penetration depth of 10 μm, i.e beyond the surface roughness *Ra* of the coating (Fig. 8).

It is remarkable from Fig. 8 that above 10 μm depth, the hardness profile varies much more regularly both in Knoop and Vickers indentations and in the same range between 1 and 3 GPa. This means that macro-indentation may be more appropriate than micro-indentation for the assessment of hardness of this kind of porous coating. In addition, the hardness obtained using Knoop indenter varies less than that obtained with the Vickers indenter.

Table 4 presents the average hardness values obtained beyond 10 μm of depth for all tests. This table shows that the average hardness values obtained with the two types of indenter are comparable. It is also noted that the standard deviation of measurement is almost identical. It

Table 4
Average hardness obtained above 10 μm depth.

Test	HP_V (GPa)	HP_K (GPa)
1	1.43 ± 0.20	1.32 ± 0.05
2	1.93 ± 0.04	1.73 ± 0.07
3	2.00 ± 0.12	1.41 ± 0.12
4	2.60 ± 0.12	1.90 ± 0.11
5	1.96 ± 0.60	2.37 ± 0.09
Average	1.98 ± 0.41	1.75 ± 0.42

seems from these results that a higher loading level, typically that encountered in macro-indentation, is better, in order to have penetration depths greater than the surface roughness. The same observation has been reported by several authors [41–43] for the characterization of rough surfaces and heterogeneous materials. These authors [41–43] have shown that a study based on statistical analysis could give an intrinsic macro-hardness value to this type of material.

Besides, Goel et al. [44] and Koshuro et al. [45] by studying Al_2O_3 plasma sprayed coatings found hardness ranging between 10 and 16 GPa depending on the spraying conditions and morphology and size of the powder feedstock which affect drastically the mechanical properties. It is clear that the obtained Vickers hardness values is around five times more that the obtained hardness in this study. This difference can be explained, on the one hand by the elaboration conditions of the

coatings and on the second hand by the conditions of hardness measurement. Indeed, Goel et al. [44] have determined the coating hardness on a polished cross-section and under only one indentation load, *i.e.* 1 N and Koshuro et al. [45] the indentation load of 2 N. In these conditions, the authors can have neglected *i*) an eventual indentation size effect (*hardness variation versus the applied load especially for lower indentation loads*), *ii*) the influence of the surface roughness on the hardness measurement (*here Ra is more than* 10 μm), *iii*) a possible release of the residual stresses due to the preparation of the sample (*cutting and polishing*), and *iv*) a probable filling of the pores resulting from the polishing. Usually, the objective is to define the mechanical properties of a coating without any change of the physical state of the coating. Subsequently the hardness must be determined on a raw sample. Under these conditions, a lower hardness number is the most often obtained, compared to hardness determination on a polished coating, resulting from the influences of the roughness, the release of the residual stress, the filling of the pores. In our opinion, the hardness thus defined is more representative of the real hardness behavior of the material, even if a large dispersion of the results is observable.

4. Conclusion

The mechanical properties of a thermally sprayed alumina coating were investigated with instrumented indentation tests using Vickers and Knoop indenters, in order to verify the methodology developed in a recent study for dense materials on porous coatings.

In this paper, it is shown that it is preferable to use multicyclic indentation tests for the characterization of porous materials with rough surface (Ra = 10.5 μm). It is highlighted that Knoop indenter seems to be more suitable for characterizing rough sprayed coating compared to the Vickers indenter due to higher contact area. The use of Knoop indenter gives more representative and homogeneous elastic modulus measurements (110 ± 40 GPa). The dispersion of elastic modulus obtained using Knoop indenter were about the half of that obtained with Vickers indentation (33% for Vickers indentation instead of 15% for Knoop indentation).

Multicyclic indentation is susceptible to introduce a densification of porous material during the test which modifies the hardness measurement (HP = 1.75 ± 0.42 GPa) which is not obvious in this work since the hardness decreases when the penetration depth increases. In addition, the hardness of the studied coating seems to depend on the indentations location. Therefore, we cannot determine an intrinsic hardness value to the coating with multicyclic indentation tests. However, it was shown that it is better to analyze the indentation data at penetration depths higher than the average height of the surface roughness *Ra*, in order to have more reliable hardness results.

Apart from these difficulties, it is shown that the methodology developed by the authors in recent study [16] for Knoop instrumented indentation on dense materials can give reliable and comparable results to those obtained with Vickers instrumented indentation on porous ceramic coating.

Declaration of competing interest

The authors declare that they have no known competing financial interests or personal relationships that could have appeared to influence the work reported in this paper.

Acknowledgements

This research was sponsored by the “Conseil Régional Nord-Pas de Calais, France” and the “Communauté d'Agglomération Maubeuge Val de Sambre CAMVS, France”.

References

[1] C.G. Levi, Emerging materials and processes for thermal barrier systems, Curr. Opin. Solid State Mater. Sci. 8 (2004) 77–91.
[2] T.J. Lu, C.G. Levi, H.N.G. Wadley, A.G. Evans, Distributed porosity as a control parameter for oxide thermal barriers made by physical vapor deposition, J. Am. Ceram. Soc. 84 (2001) 2937–2946 12.
[3] J. Singh, D.E. Wolfe, R.A. Miller, J.I. Eldridge, D.-M. Zhu, Tailored microstructure of zirconia and hafnia-based thermal barrier coatings with low thermal conductivity and high hemispherical reflectance by EB-PVD, J. Mater. Sci. 39 (2004) 1975–1985.
[4] A. Leyland, A. Matthews, On the significance of the H/E ratio in wear control: a nanocomposite coating approach to optimised tribological behaviour, Wear 246 (2000) 1–11.
[5] P. Clément, S. Meille, J. Chevalier, C. Olagnon, Mechanical characterization of highly porous inorganic solids materials by instrumented micro-indentation, Acta Mater. 61 (2013) 6649–6660.
[6] Y. An, S. Li, G. Hou, X. Zhao, H. Zhou, J. Chen, Mechanical and tribological properties of nano/micro composite alumina coatings fabricated by atmospheric plasma spraying, Ceram. Int. 43 (2017) 5319–5328.
[7] G. Di Girolamo, A. Brentari, C. Blasi, E. Serra, Microstructure and mechanical properties of plasma sprayed alumina-based coatings, Ceram. Int. 40 (2014) 12861–12867.
[8] P. Ctibor, P. Bohac, M. Stranyanek, R. Ctvrtlık, Structure and mechanical properties of plasma sprayed coatings of titania and alumina, J. Eur. Ceram. Soc. 26 (2006) 3509–3514.
[9] D. Chicot, H. Ageorges, M. Voda, G. Louis, M.A. Ben Dhia, C.C. Palacio, S. Kossman, Hardness of thermal sprayed coatings: relevance of the scale of measurement, Surf. Coating. Technol. 268 (2015) 173–179.
[10] š. Houdková, M. Kašparová, Experimental study of indentation fracture toughness in HVOF sprayed hardmetal coatings, Eng. Fract. Mech. 110 (2013) 468–476.
[11] S. Karthikeyan, V. Balasubramanian, R. Rajendran, Developing empirical relationships to estimate porosity and Young's modulus of plasma sprayed YSZ coatings, Appl. Surf. Sci. 296 (2014) 31–46.
[12] J. Nohava, R. Mušálek, J. Matějíček, M. Vilémová, A contribution to understanding the results of instrumented indentation on thermal spray coatings — case study on Al2O3 and stainless steel, Surf. Coating. Technol. 240 (2014) 243–249.
[13] D. Jauffrès, C. Yacou, M. Verdier, R. Dendievel, A. Ayral, Mechanical properties of hierarchical porous silica thin films: experimental characterization by nanoindentation and Finite Element modeling, Microporous Mesoporous Mater. 140 (2011) 120–129.
[14] G.R. Anstis, P. Chantikul, B.R. Lawn, D.B. Marshall, A critical evaluation of indentation techniques for measuring fracture toughness: I, direct crack measurements, J. Am. Ceram. Soc. 64 (1981) 533–538 9.
[15] S.J. Bull, Analysis methods and size effects in the indentation fracture toughness assessment of very thin oxide coatings on glass, Compt. Rendus Mec. 339 (2011) 518–531.
[16] G. Ben Ghorbal, A. Tricoteaux, A. Thuault, G. Louis, D. Chicot, Mechanical characterization of brittle materials using instrumented indentation with Knoop indenter, Mech. Mater. 108 (2017) 58–67.
[17] L. Riester, P.J. Blau, E. Lara-Curzio, K. Breder, Nanoindentation with a Knoop indenter, Thin Solid Films 377 (2000) 635–639.
[18] L. Riester, T.J. Bell, A.C. Fischer-Cripps, Analysis of depth-sensing indentation tests with a Knoop indenter, J. Mater. Res. 16 (2001) 1660–1667.
[19] D. Chicot, E. Bemporad, G. Galtieri, F. Roudet, M. Alvisi, J. Lesage, Analysis of data from various indentation techniques for thin films intrinsic hardness modelling, Thin Solid Films 516 (2008) 1964–1971.
[20] R. Saha, W.D. Nix, Effects of the substrate on the determination of thin film mechanical properties by nanoindentation, Acta Mater. 50 (2002) 23–38.
[21] ISO 14577:2015, *Metallic materials — instrumented indentation test for* Hardness and Materials Parameters — Part 1: Test Method — Part 2: Verification and Calibration of Testing Machines — Part 3: Calibration of Reference Blocks.
[22] M. Miller, C. Bokko, M. Vandamme, F.J. Ulm, Surface roughness criteria for cement paste nanoindentation, Cement Concr. Res. 38–4 (2008) 467–476.
[23] K. Jankowski, A. Wymysłowski, D. Chicot, Combined loading and failure analysis of lead-free solder joints due to creep and fatigue phenomena, Solder. Surf. Mt. Technol. 26–1 (2014) 22–26.
[24] A. Mejias, R.T. Candidato, L. Pawłowski, D. Chicot, Mechanical properties by instrumented indentation of solution precursor plasma sprayed hydroxyapatite coatings: analysis of microstructural effect, Surf. Coating. Technol. 298 (2016) 93–102.
[25] D. Chicot, F. Roudet, A. Zaoui, G. Louis, V. Lepingle, Influence of visco-elasto-plastic properties of magnetite on the elastic modulus: multicyclic indentation and theoretical studies, Mater. Chem. Phys. 119 (2010) 75–81.
[26] W.C. Oliver, G.M. Pharr, Measurement of hardness and elastic modulus by instrumented indentation: advances in understanding and refinements to methodology, J. Mater. Res. 19 (2004) 3–20.
[27] W.C. Oliver, G.M. Pharr, An improved technique for determining hardness and elastic modulus using load and displacement sensing indentation experiments, J. Mater. Res. 7 (1992) 1564–1583.
[28] I.N. Sneddon, The relation between load and penetration in the axisymmetric Boussinesq problem for a punch of arbitrary profile, Int. J. Eng. Sci. 3 (1965) 47–57.
[29] J.C. Hay, A. Bolshakov, G.M. Pharr, A critical examination of the fundamental relations used in the analysis of nanoindentation data, J. Mater. Res. 14 (1999) 2296–2305.
[30] G. Ben Ghorbal, A. Tricoteaux, A. Thuault, G. Louis, D. Chicot, Comparison of

conventional Knoop and Vickers hardness of ceramic materials, J. Eur. Ceram. Soc. 37 (2017) 2531–2535.
[31] A.E. Giannakopoulos, Th Zisis, Analysis of Knoop indentation, Int. J. Solid Struct. 48 (2011) 175–190.
[32] D.B. Marshall, T. Noma, A.G. Evans, A simple method for determining elastic-modulus-to-hardness ratios using Knoop indentation measurements, J. Am. Ceram. Soc. 65 (1982) c175–c176.
[33] G.M. Pharr, A. Bolshakov, Understanding nanoindentation unloading curves, J. Mater. Res. 17 (2002) 2660–2671.
[34] A.C. Fischer-Cripps, Critical review of analysis and interpretation of nanoindentation test data, Surf. Coating. Technol. vol. 200, (2006) 4153–4165.
[35] L. Łatka, D. Chicot, A. Cattini, L. Pawłowski, A. Ambroziak, Modeling of elastic modulus and hardness determination by indentation of porous yttria stabilized zirconia coatings, Surf. Coating. Technol. 220 (2013) 131–139.
[36] T.Y. Tsui, J. Vlassak, W.D. Nix, Indentation plastic displacement field: Part I. The case of soft films on hard substrates, J. Mater. Res. 14 (1999) 2196–2203.
[37] J. Thurn, D.J. Morris, R.F. Cook, Depth-sensing indentation at macroscopic dimensions, J. Mater. Res. 17 (2002) 2679–2690.
[38] E. Gregorová, W. Pabst, V. Nečina, T. Uhlířová, P. Diblíková, Young's modulus evolution during heating, re-sintering and cooling of partially sintered alumina ceramics, J. Eur. Ceram. Soc. 39 (2019) 1893–1899.
[39] J. Gong, J. Wang, Z. Guan, A comparison between Knoop and Vickers hardness of silicon nitride ceramics, Mater. Lett. 56 (2002) 941–944.
[40] S.J. Bull, On the origins and mechanisms of the indentation size effect, Z. Metallkd. 94 (2003) 787–792.
[41] F.-J. Ulm, M. Vandamme, C. Bobko, J. Alberto Ortega, K. Tai, C. Ortiz, Statistical indentation techniques for hydrated nanocomposites: concrete, bone, and shale, J. Am. Ceram. Soc. 90 (2007) 2677–2692.
[42] Y. Xia, M. Bigerelle, S. Bouvier, A. Iost, P.-E. Mazeran, Quantitative approach to determine the mechanical properties by nanoindentation test: application on sandblasted materials, Tribol. Int. 82 (2015) 297–304.
[43] J.-M. Schneider, M. Bigerelle, A. Iost, Statistical analysis of the Vickers hardness, Mater. Sci. Eng., A 262 (1999) 256–263.
[44] S. Goel, S. Björklund, N. Curry, U. Wiklund, S.V. Joshi, Axial suspension plasma spraying of Al2O3 coatings for superior tribological properties, Surf. Coating. Technol. 315 (2017) 80–87.
[45] V. Koshuro, A. Fomin, I. Rodionov, Composition, structure and mechanical properties of metal oxide coatings produced on titanium using plasma spraying and modified by micro-arc oxidation, Ceram. Int. 44 (2018) 12593–12599 11.